Rev. Roum. Sci. Techn.– Électrotechn. et Énerg.
Vol. **69**, *3*, pp. 269–276, Bucarest, 2024

INTELLIGENT FAULT DETECTION AND LOCATION IN ELECTRICAL HIGH-VOLTAGE TRANSMISSION LINES

KHALED GUERRAICHE[1], AMINE BOUADJMI ABBOU[1], LATIFA DEKHICI[2,1]

Keywords: Machine Learning; Fault location; Optimization; Atom search optimization; Transmission lines.

Fault location in transmission lines is critical to ensure the power systems' reliable and efficient operation. Accurate fault detection and localization are essential to minimize downtime, prevent cascading failures, and maintain the overall stability of the electrical grid. Over the years, various fault location methods have been proposed, ranging from traditional model-based approaches to more sophisticated artificial intelligence techniques. This research presents two fault location methodologies: the Atom search optimization metaheuristic approach (ASO) and machine learning (ML) with cubic spline models. We evaluate the performance of both approaches by considering different fault types, fault distances, and fault resistance. We analyze accuracy and computational efficiency. The findings reveal that the Metaheuristic Approach demonstrates robustness in fault detection and localization under diverse conditions but may suffer from higher computational overhead. In contrast, the hybridization of machine learning and metaheuristic exhibits promising potential in achieving real-time fault localization with improved accuracy.

1. INTRODUCTION

With the ever-increasing demand for reliable and stable power supply, efficient fault location techniques have become paramount in modern power systems. Power system faults, such as short-circuits and line failures, can lead to widespread outages and economic losses and even jeopardize public safety. Therefore, timely and accurate fault location is of utmost importance to swiftly restore power and minimize the impact of disruptions. Traditional fault location methods, like impedance-based techniques, have been reliable tools for decades. However, with power systems' growing complexity and size, conventional approaches face limitations in handling intricate network structures and large-scale systems.

In recent years, significant advancements in computational intelligence and data-driven methods have led to integrating metaheuristic algorithms and machine learning techniques in fault location practices. These tools effectively address the non-linearity and high dimensional challenges inherent in fault location within power systems. They can effectively search for optimal or near-optimal solutions in a vast solution space, enabling more accurate and efficient fault location. On the other hand, the rapid growth of machine learning has opened new possibilities in various fields, including power system fault diagnosis. Machine learning techniques have remarkably succeeded in pattern recognition, classification, and regression tasks, particularly supervised and unsupervised. Leveraging historical data from power systems, machine learning models can learn intricate fault patterns and accurately identify fault locations. Integrating metaheuristic algorithms and machine learning techniques in fault location brings forth a synergistic approach that combines the robust optimization capabilities of metaheuristics with the data-driven insights of machine learning. This amalgamation has the potential to revolutionize fault location practices in power systems and enhance their reliability and resilience.

Recently, numerous approaches have been proposed for pinpointing fault locations in electrical lines. Harmony search (HS) and teaching learning-based optimization (TLBO) techniques for fault location estimation in two-terminal transmission lines [1]. The fault location method employs Field programmable gate array (FPGA) combined with artificial neural networks (ANN) theory [2]. Linear optimization methods like the simplex method and Nelder-Mead, which are applied by [3]. Harmony search optimization for estimating fault distance in simulated cases [4]. Genetic algorithms are implemented [5] to compare waveforms from digital fault recorders with simulated waves. Fault location approach for VSC-HVDC Systems based on NSGA-II and discrete wavelet transform [6]. An optimization-based fault location algorithm for series-compensated power transmission lines [7]. A Category boosting machine learning algorithm for breast cancer prediction [8].

Reference [9] suggested that using automatic feature extraction by transfer learning has shown promising results in transmission line protection. This approach has been applied in various fields, including wind turbine fault modeling and classification using cuckoo-optimized modular neural networks [10] and deep vein thrombosis identification via the deep vein net, a deep learning network optimized by the sooty tern algorithm [11]. Additionally, real-time diagnosis of battery cells for stand-alone photovoltaic systems using machine learning techniques has been explored [12]. Another novel fault location technique for transmission lines utilizes positive sequence signals in a single-ended manner [13].

This paper presents a comprehensive survey of state-of-the-art research on fault location in power systems, focusing specifically on utilizing atom search optimization metaheuristic [14] and machine learning methods with cubic spline models [15]. We aim to explore the various applications of these techniques, evaluate their performance in different scenarios, and highlight their advantages and limitations. This method is implemented on a system comprising two generators connected to a high-voltage transmission line to assess its operational performance.

The paper's structure is organized as follows: section 3 introduces the mathematical formulation of fault location, followed by an in-depth discussion of the application of atom search optimization and machine learning techniques in fault location. Subsequently, section 4 presents the simulation results. Finally, section 5 concludes the paper by summarizing the key findings and emphasizing the significance of integrating metaheuristic and machine learning approaches for fault location in power systems.

[1] LDREI Laboratory, Department of Electrical Engineering, Higher School of Electrical Engineering and Energetic, Oran, Algeria
E-mails: guerraiche_khaled@esgee-oran.dz; abbou_aminebouadjmi@esgee-oran.dz
[1,2] Faculty of Computer Sciences, University of Sciences and Technology of Oran, Algeria. E-mails: latifa.dekhici@univ-usto.dz

DOI: 10.59277/RRST-EE.2024.69.3.2

By exploring the cutting-edge research and advancements in this domain, this paper seeks to shed light on the promising path forward for fault location methodologies, empowering power system engineers and operators with innovative tools to maintain the stability and reliability of modern power grids.

2. MATHEMATICAL FORMULATION OF FAULT LOCATION

Assume that a fault has taken place at point L along the transmission line as shown in Fig. 1. It is possible to deduce the fault point's voltage in terms of the measured parameters at terminal A [16]. The Fig. 2, shows a single-phase transmission.

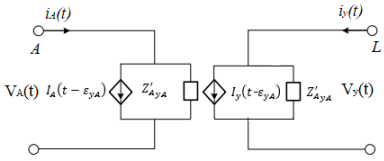

Fig. 1 – Illustrates the distributed time domain model for the AL segment.

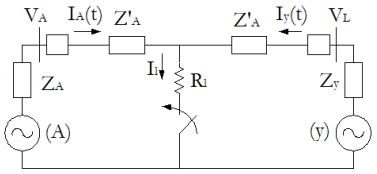

Fig. 2 – Single-phase representation of the transmission line.

Equation 1 combines the effects of delayed voltages and currents, as well as resistive losses, to determine the voltage $V_{yA}(t)$ at a specific point in the network at time t. It considers propagation delays and the complex interactions between network elements, thereby allowing for precise modeling of electromagnetic transients.

$$V_{yA}(t) = \frac{1}{2(Z_A)^2}\{\left(Z'^{\,2}_{A_{yA}}\right)\left[V_A(t-\varepsilon_{yA}) - Z'_{AyA}i_A(t-\varepsilon_{yA})\right] + \left(Z''^{\,2}_{A_{yA}}\right)\left[V_A(t-\varepsilon_{yA}) + Z''_{AyA}i_A(t-\varepsilon_{yA})\right] - \frac{R_{yA}^2}{8}V_A(t) - \frac{R_{yA}}{2}Z'_{AyA}Z''_{AyA}i_A(t)\}. \quad (1)$$

Using a comparable method, the voltage at the fault location can be represented in terms of the data recorded at terminal B [6]:

$$V_{yB}(t) = \frac{1}{2(Z_A)^2}\{\left(Z'^{\,2}_{A_{yB}}\right)\begin{bmatrix} V_B\left(t+(T-\varepsilon_{yA})\right) \\ -Z'_{AyB}i_B\left(t+(T-\varepsilon_{yA})\right)\end{bmatrix} + \left(Z''^{\,2}_{A_{yB}}\right)\left[V_B\left(t-(T-\varepsilon_{yA})\right) + Z''_{AyB}i_B\left(t-(T-\varepsilon_{yA})\right)\right]. \quad (2)$$

wherein: R_{yB} – resistance of the BL segment, $Z'_{AyB} = Z_A + \frac{R_{yB}}{4}$, $Z''_{AyB} = Z_A - \frac{R_{yB}}{4}$; T is a time required for the wave to propagate from the sending end (A) to the receiving end (B). Given that the fault point's voltage should remain consistent regardless of the data used for its calculation, the two obtained voltages, V_{yA} and V_{yB}, must be equivalent across all sampling instances.

As a result, the following equation must hold true at the actual fault point (L) for all moments [16]:

$$F\left(V_A, i_A, V_B, i_B, t, \varepsilon_{yA}\right) = V_{yA}(t) - V_{yB}(t) = 0. \quad (3)$$

The distance from the sending terminal (A) to the fault point, denoted as *y*, is not overtly present in (3), it's embedded within the surge travel time, ε_{yA}. Additionally, this travel time isn't explicitly listed as a variable in this equation; rather, it's a value upon which the voltages and currents rely [16]:

$$\text{in objective function } \left(n_{yA}\right) = \sum_{k=n_{yA}}^{N-n_{yA}} FO^2\left(n_{yA}, p\right). \quad (4)$$

where: $n_{yA} = \frac{\varepsilon_{yA}}{\Delta t}$, $p = \frac{t}{\Delta t}$, N = total samples, Δt sampling time, n_{yA}, p = arbitrary integers.

The elusive fault location is determined through the minimization of the defined objective function. To elaborate further, the initial step involves calculating the value of the subsequent equation for every potential fault location [16]:

$$\sum_p FO^2(k) = \sum_p \left[V_{yA}(p) - V_{yB}(p)\right]^2. \quad (5)$$

At the real fault location, (5) should reach its lowest value. Consequently, this value must be computed for every potential fault location along the transmission line. Among all these potential locations, the one where (5) attains the minimum value is chosen as the true fault location.

In this proposed approach, atomic search optimization (ASO) is employed to minimize the objective function. Section 3.1 will provide further elaboration on this.

3. ALGORITHM FOR DETERMINING FAULT LOCATION

This section utilizes two distinct methodologies: Atom search optimization (ASO) and machine learning. ASO, a nature-inspired optimization technique, emulates the behavior of atoms in chemical reactions to explore solution spaces efficiently. ASO's ability to perform global optimization makes it a valuable candidate for addressing complex optimization problems. On the other hand, machine learning, a data-driven approach, leverages algorithms to identify patterns and relationships within data, enabling the model to make informed predictions or decisions. The integration of ASO and machine learning holds promise in enhancing the accuracy and efficiency of solution processes by harnessing the strengths of both methods. This section elaborates on the synergistic use of ASO and machine learning to achieve enhanced performance and more robust outcomes in the context of the studied problem.

3.1. ATOM SEARCH METHOD

The atom search optimization (ASO) method, proposed by Weiguo Zhao [14], operates based on mimicking the interactions between atoms in chemical reactions to perform optimization tasks. ASO introduces atoms as agents that search for optimal solutions by moving within a solution space. Each atom is assigned a position, and their movements are influenced by their energy levels, which are determined by the objective function being optimized. The atoms' behaviors are guided by various forces, including atomic forces, metallic attraction, and van der Waals forces, all of which drive them toward better solutions. Weiguo Zhao [14], innovative approach combines principles from chemistry and optimization to create an efficient algorithm capable of tackling complex optimization problems. This fusion of scientific concepts from different domains underpins the ASO method's effectiveness and underscores modern optimization techniques' interdisciplinary nature. Atoms maintain varying distances from each other, experiencing reciprocal forces of attraction and repulsion.

3.2. MACHINE LEARNING METHOD

Machine learning enables computers to learn from data and progressively enhance their performance without being

explicitly programmed. It revolves around the concept of algorithms identifying patterns, extracting insights, and making predictions based on input data. The process generally involves three key components: data, a model, and an optimization algorithm. Initially, a dataset is collected, encompassing relevant features and corresponding outcomes. The model, often a mathematical representation, is then developed to capture relationships within the data. Through an iterative process, the model is refined using an optimization algorithm that adjusts its parameters to minimize the difference between predicted outcomes and actual data. This continuous iteration, known as training, fine-tunes the model's performance. Once the model is trained, it can be deployed to make predictions on new, unseen data. As more data becomes available, the model can adapt and improve its predictions, showcasing the self-learning aspect of machine learning. The efficacy of machine learning hinges on its capability to generalize from training data to make accurate predictions on new, unseen instances, effectively automating complex tasks and uncovering insights that might be challenging for traditional rule-based programming.

Applying machine learning techniques has brought significant advancements to fault localization in high-voltage transmission lines. With these power systems' complex and expansive nature, accurate and timely identification of faults is crucial for ensuring reliable and efficient operation. Machine learning approaches, driven by their ability to process extensive datasets and discern intricate patterns, have proven invaluable in enhancing fault detection and localization processes. This paper delves into the utilization of machine learning algorithms to improve the accuracy and speed of fault localization in high-voltage transmission lines, shedding light on the innovative solutions they offer to tackle the challenges posed by these critical infrastructure components.

3.2.1. Collecting data

Collecting data for machine learning, specifically targeted at fault detection in a 300 km long electrical transmission line with variable fault resistances ranging from 1 to 50 Ω, requires a careful and strategic approach. To ensure the effectiveness of the model, the data collection process should encompass a wide range of fault scenarios that reflect the real-world conditions the model will encounter. This involves creating synthetic faults across the entire length of the transmission line, varying the resistance values within the specified range. The dataset should also include a diversity of fault types, such as single-phase to earth fault, isolated two-phase/to earth and three-phase, to ensure the model's versatility. For a fault resistance range of 0 to 50 Ω with a step size of 1 Ω, a transmission line spanning 300 km with a step size of 1 km, and a voltage range of ±10 % between the two terminals with a step size of 1 kV, we would have a total of 51×299×80×80, resulting in 97 593 600 simulations required for data collection. However, this extensive number of simulations proves unfeasible for standard computing capabilities. The solution in this context is to strategically select the most influential variables that lead to minimal error during the localization process.

If we take $V_A = V_B = V$ we will have just 1 219 920 simulations to do to collect the data. The short-circuit current can be modeled as a function depending on the supply voltage, resistance and fault distance parameters. So, there are three variables that influence the short-circuit current value.

The pseudocode for data collection for all types of faults is mentioned in Fig. 3.

Machine learning algorithm

```
Enter N = (Nominal voltage × 10% × 2) / Step, where Step is the voltage
increment step, and the optimal step is 1 kV.
Enter M, the maximum desired value of fault resistance, and Step R, which
is the resistance increment step, with the optimal step being 1 Ω.
Enter l, the total distance of the transmission line in kilometers, with the
optimal step being 1 km.
For i = 1:N
    If i = 1
      V = Nominal voltage - (Nominal voltage * 10%)
    Else
      V = V + Step
    End If
        For j = 1:(M+1)/Step R
            If j = 1
              RF = 0 Ω
            Else
              RF = RF + Step R
            End If
                For dis = 1:l
                    Fault distance = dis
                    Perform a simulation for V, RF, and l for each
iteration i, j, and dis.
                    Collect current data for V, RF, and l for each
iteration i, j, and dis.
                End dis = 1:l
      End j = 1:(M+1)/Step R
End i = 1:N
End Program.
```

Fig. 3 – Pseudocode for data collection for all types of faults.

4. RESULTS

This section assesses the effectiveness of the presented algorithms. The illustration in Fig. 4, depicts a 400 kV three-phase transmission line spanning 300 km. A fault emerges at an arbitrary location L and positioned at a distance x from the sending end (A terminal).

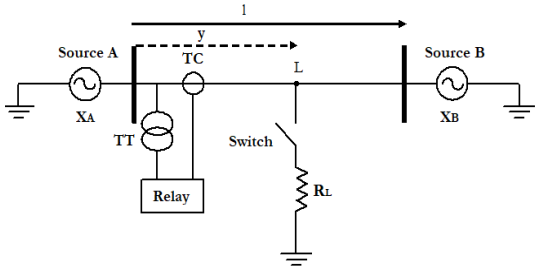

Fig. 4 – Protection system and its attributes.

Utilising MATLAB/Simulink software, the measurements are extracted and then imported into the atom search algorithm and machine learning with MATLAB. The precision of the introduced fault location technique has been assessed for both symmetric and asymmetric faults across various fault positions, and the error percentage, computed according to (6), is outlined in Table 1, 2 and 3

$$e(\%) = \left|\frac{y_{comp} - y_{real}}{l_{AB}}\right| \times 100 \qquad (6)$$

y_{comp} – computed fault position, y_{real} – real fault location, l_{AB} – entire length of the transmission line.

Figures 5, 6, and 7 illustrate the effect of different fault locations along the transmission line with various fault resistance values, R_L = 1, 10, and 50 Ω. As the fault moves further from the relay, the detection accuracy is affected, increasing the error for TLBO and HS with almost negligible values.

Table 1

Location results for the different methods for a fault resistance R_L= 1 Ω

R_L = 1 Ω

Fault Type	Real Fault Location (km)	TLBO [1]		HS [1]		ASO		ML (spline)	
		Computed distance (km)	Error (%)	Computed distance (km)	Error (%)	Computed distance (km)	Error (%)	Computed distance (km)	Error (%)
ABCG	5	4.986	0.0046	5.095	0.0316	5.0133	0.0044	5	1.0136e-06
	25	24.928	0.024	24.947	0.0177	25.0112	0.0037	25	4.3631e-06
	50	49.857	0.048	49.906	0.0314	49.967	0.0109	50	1.6448e-05
	100	99.99	0.0033	100.471	0.01571	99.9618	0.0127	99.9998	5.1666e-05
	150	150.13	0.133	150.236	0.0786	149.9842	0.0052	149.9998	8.0225e-05
	200	199.979	0.0069	200.351	0.1170	199.979	0.0070	199.9998	8.3007e-05
	250	250.389	0.1296	250.351	0.1038	249.9737	0.0087	249.9999	4.2674e-05
	275	275.152	0.0507	275.511	0.1702	274.9849	0.0050	275	2.6527e-13
	295	294.985	0.0050	294.990	0.0033	294.9828	0.0057	295.0002	5.2678e-05
ABG	5	5.073	0.0244	5.299	0.0998	4.9856	0.0047	5	6.9747e-06
	25	24.928	0.0240	24.721	0.0931	24.9558	0.0147	25	6.8186e-06
	50	49.860	0.0467	50.10	0.0334	50.0224	0.0074	50	4.737e-15
	100	99.991	0.0031	100.1826	0.0609	99.9618	0.0127	99.9999	2.2147e-05
	150	150.396	0.1320	150.2943	0.0981	149.9842	0.0052	149.9999	3.8613e-05
	200	200.041	0.0137	200.063	0.0210	199.979	0.0070	199.9999	3.0611e-05
	250	250.370	0.1233	250.646	0.2115	250.0291	0.0097	250.0001	1.8686e-05
	275	275.19	0.0632	274.419	0.0193	274.9295	0.0234	275.0002	5.6075e-05
	295	294.997	0.0010	294.83	0.00551	294.9551	0.0149	295.0002	5.4908e-05
AG	5	4.992	0.0028	5.032	0.0105	4.3209	0.2263	5	5.8302e-06
	25	24.98	0.0067	25.246	0.0821	25.0073	0.0024	25	5.6568e-06
	50	49.86	0.048	50.204	0.0680	49.9956	0.0014	50	0
	100	99.993	0.0023	100.0303	0.0101	99.9722	0.0092	99.9999	2.0447e-05
	150	150.13	0.04	150.2967	0.0989	149.9677	0.0107	149.9999	3.6611e-05
	200	199.996	0.0015	200.131	0.0436	199.9823	0.0059	199.9999	2.7689e-05
	250	250.128	0.0427	250.441	0.1469	249.9968	0.0010	250	1.3079e-05
	275	275.044	0.013	275.121	0.0402	274.9851	0.0049	275.0001	2.6178e-05
	295	295.005	0.0016	295.13	0.0438	295.0382	0.0127	295	1.3388e-05
AB	5	4.986	0.0048	4.762	0.0793	4.8748	0.0417	5	9.2963e-06
	25	24.928	0.0240	24.721	0.0931	24.9835	0.0054	25	7.4072e-06
	50	49.860	0.0467	50.10	0.0334	50.0224	0.0074	50	4.737e-15
	100	99.991	0.0031	100.1826	0.0609	99.9618	0.0127	99.9999	2.236e-05
	150	150.396	0.1320	150.2943	0.0981	149.9842	0.0052	149.9999	3.8559e-05
	200	200.041	0.0137	200.063	0.0210	199.979	0.0070	199.9999	3.0179e-05
	250	250.370	0.1233	250.646	0.2115	250.0291	0.0097	250.0001	1.8377e-05
	275	275.19	0.0632	274.419	0.0193	274.9572	0.0142	275.0002	6.0355e-05
	295	294.983	0.0057	294.91	0.0287	295.149	0.0496	295.0003	9.9253e-05

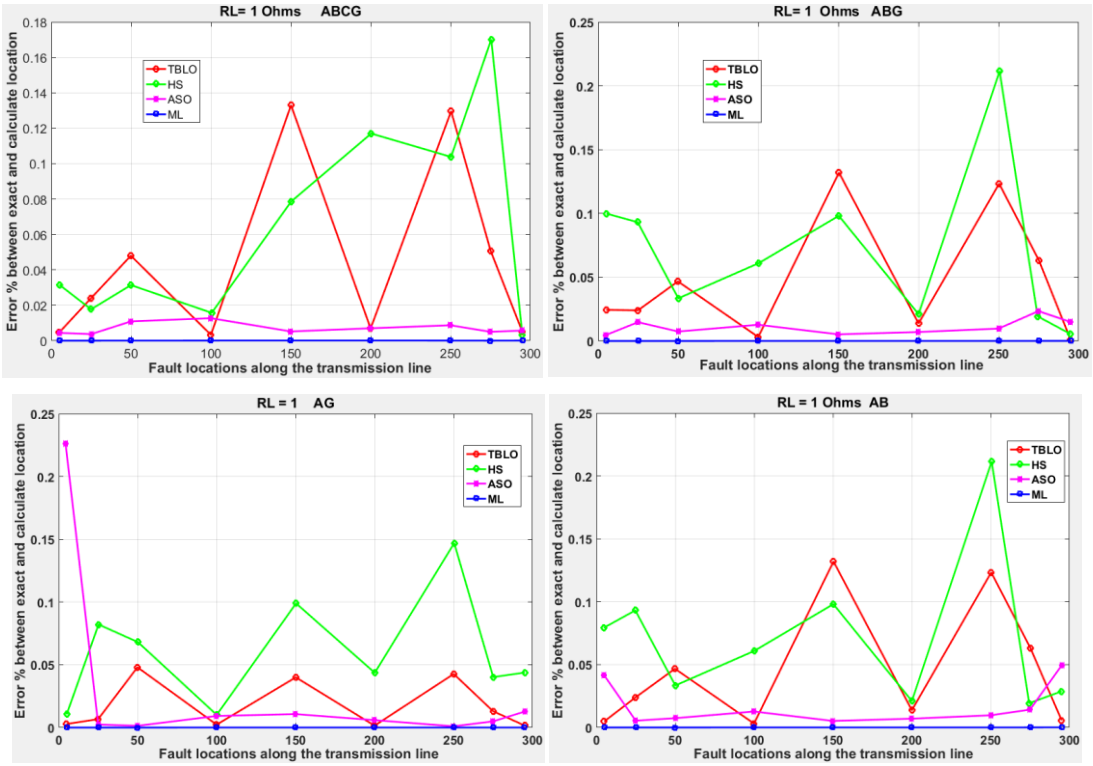

Fig. 5 – TBLO, HS, ASO, and ML fault location results along the transmission line with different fault locations and fault resistance R_L = 1 Ω.

Table 2
Location results for the different methods for a fault resistance R_L= 10 Ω.

R_L = 10 Ω

Fault Type	Real Fault Location (km)	TLBO [1]		HS [1]		ASO		ML (spline)	
		Computed distance (km)	Error (%)	Computed distance (km)	Error (%)	Computed distance (km)	Error (%)	Computed distance (km)	Error (%)
ABCG	5	5.03	0.0099	5.0329	0.0110	5.041	0.0136	5	1.3304e-06
	25	24.928	0.024	25.0435	0.0145	24.9835	0.0054	25	4.2513e-06
	50	49.856	0.048	49.6299	0.0123	49.967	0.0109	50	1.4122e-05
	100	99.989	0.0036	100.1268	0.0423	99.9618	0.0127	99.9999	4.3301e-05
	150	150.3761	0.1253	150.3181	0.1060	149.9842	0.0052	149.9998	7.8879e-05
	200	199.9814	0.0062	200.123	0.0410	199.979	0.0070	199.9998	7.3405e-05
	250	250.3839	0.1279	250.433	0.01443	250.0291	0.0097	249.9999	2.491e-05
	275	275.2921	0.096	275.395	0.1317	275.0126	0.0042	275	1.3263e-13
	295	294.983	0.0056	295.254	0.0848	295.0936	0.0312	295	6.1094e-06
ABG	5	5.021	0.0099	4.834	0.0553	4.9856	0.0047	5	1.5113e-05
	25	24.931	0.024	25.535	0.1783	25.0112	0.0037	25	9.1017e-06
	50	49.856	0.048	50.0201	0.0067	49.967	0.0109	50	1.1842e-13
	100	99.994	0.0036	100.2034	0.0678	99.9618	0.0127	99.9999	2.3032e-05
	150	150.3759	0.1253	150.3168	0.1056	149.9842	0.0052	149.9999	3.8164e-05
	200	200.0283	0.0062	200.0758	0.0253	199.979	0.0050	199.9999	2.6568e-05
	250	250.353	0.1279	249.922	0.0261	250.0014	0.0004	250	1.0714e-05
	275	275.289	0.096	275.103	0.0344	274.9849	0.0050	275.0001	2.1817e-05
	295	295.010	0.0056	295.184	0.0614	294.8721	0.0426	295.0001	1.9522e-05
AG	5	4.987	0.0046	5.0667	0.0222	3.7669	0.4110	5	9.6784e-06
	25	24.935	0.0215	25.6832	0.2277	24.9314	0.0228	25	6.8001e-06
	50	49.89	0.048	49.9177	0.0274	49.9386	0.0204	50	4.737e-14
	100	100.021	0.0070	100.0644	0.0215	99.9722	0.0092	99.9999	2.0888e-05
	150	150.396	0.13	150.1103	0.0368	149.9867	0.0044	149.9999	3.6611e-05
	200	200.0686	0.0228	200.1462	0.0487	199.9823	0.0059	199.9999	2.6468e-05
	250	250.3688	0.1229	250.134	0.0447	250.0158	0.0052	250	1.0754e-05
	275	275.289	0.096	275.302	0.1006	275.023	0.0076	275.0001	1.789e-05
	295	294.983	0.0056	295.254	0.0117	295.0213	0.0070	295	8.1369e-06
AB	5	5.027	0.009	5.0329	0.0110	5.041	0.0136	5	1.597e-05
	25	24.956	0.024	25.1255	0.0418	24.9835	0.0054	25	9.8314e-06
	50	49.874	0.048	50.059	0.0197	49.967	0.0109	50	1.1606e-13
	100	99.995	0.0036	99.987	0.0045	99.9618	0.0127	99.9999	2.3615e-05
	150	150.399	0.1253	150.190	0.0633	149.9565	0.0144	149.9999	3.8273e-05
	200	199.983	0.0062	200.218	0.0726	199.979	0.0070	199.9999	2.7118e-05
	250	250.377	0.1279	250.536	0.1788	250.0014	0.0004	250	1.1928e-05
	275	275.291	0.096	275.145	0.0485	274.9572	0.0142	275.0001	2.4467e-05
	295	294.990	0.0056	295.254	0.0847	294.9551	0.0149	295.0001	1.9893e-05

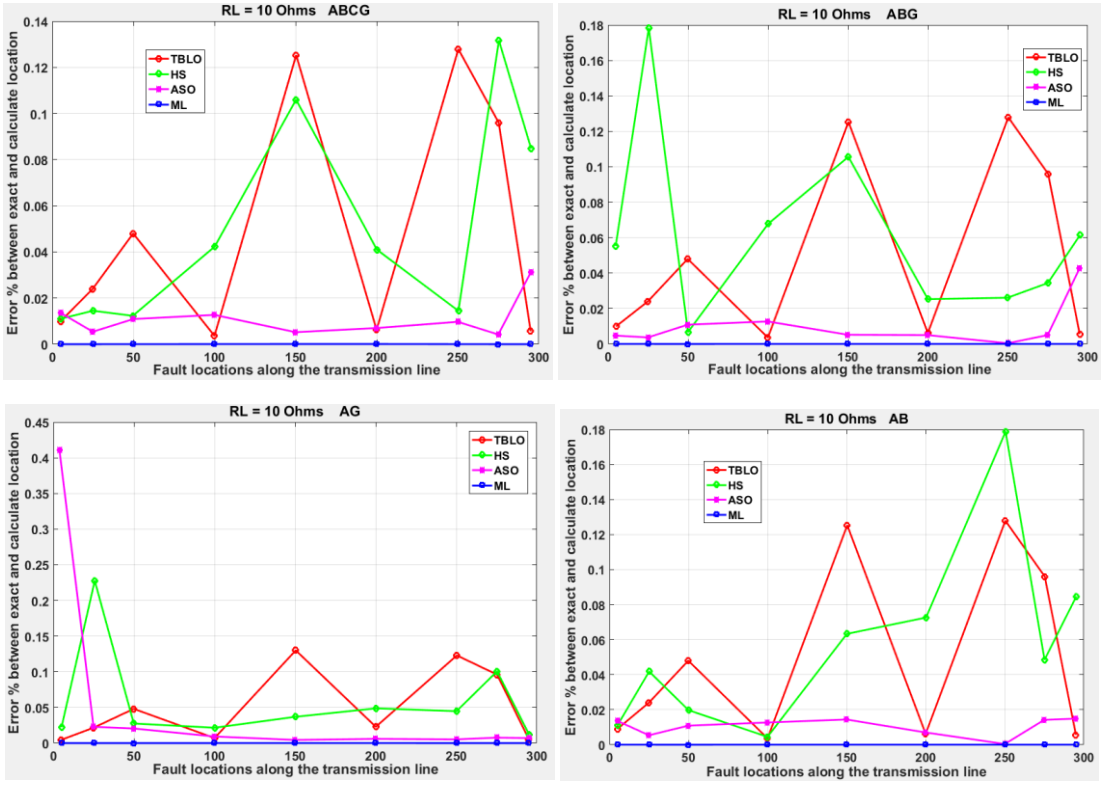

Fig. 6 – TBLO, HS, ASO, and ML fault location results along the transmission line with different fault locations and fault resistance R_L = 10 Ω.

Table 3

Location results for the different methods for a fault resistance R_L= 50 Ω

		R_L = 50 Ω							
Fault Type	Actual Fault Location (km)	TLBO [1]		HS [1]		ASO		ML (spline)	
		Computed distance (km)	Error (%)	Computed distance (km)	Error (%)	Computed distance (km)	Error (%)	Computed distance (km)	Error (%)
ABCG	5	5.125	0.0416	5.0576	0.0192	4.9302	0.0232	5	6.9052e-06
	25	25.204	0.0679	25.0026	0.0009	24.9004	0.0331	25	1.594e-05
	50	50.109	0.0362	50.0751	0.0250	49.9393	0.0202	49.9999	3.7436e-05
	100	99.9905	0.0036	100.017	0.0057	99.9895	0.0035	99.9998	6.7968e-05
	150	150.1296	0.0432	150.1721	0.0574	149.9842	0.0052	149.9998	7.0659e-05
	200	199.9796	0.007	199.9816	0.0061	199.979	0.0070	199.9999	3.8344e-05
	250	250.1861	0.062	250.485	0.1615	249.9737	0.0087	250	7.8055e-06
	275	275.2256	0.0752	275.568	0.1893	275.0126	0.0042	275	4.737e-13
	295	294.983	0.0056	295.233	0.0775	299.9131	1.6377	295	9.1599e-07
ABG	5	5.119	0.0396	5.487	0.1624	4.9302	0.0232	5.0002	5.8874e-05
	25	25.203	0.0677	25.2774	0.0925	24.9558	0.01473	25.0001	2.7512e-05
	50	50.132	0.0439	50.2442	0.0814	49.9393	0.0202	50	1.6106e-12
	100	99.997	0.0010	100.7873	0.2624	99.9618	0.0127	99.9999	3.1875e-05
	150	150.1317	0.0439	150.0306	0.0102	149.9842	0.0052	149.9999	3.5902e-05
	200	199.98	0.0067	200.2698	0.0899	199.979	0.0070	199.9999	1.6884e-05
	250	250.172	0.0573	250.335	0.1115	249.946	0.0179	250	4.8321e-06
	275	275.2012	0.0671	274.504	0.1654	274.9849	0.0050	275	8.6834e-06
	295	295.006	0.0020	295.002	0.0006	299.9408	1.6469	295	6.3537e-06
AG	5	4.969	0.0103	4.8292	0.0569	4.9711	0.0096	5.0001	4.6124e-05
	25	25.064	0.0214	25.3089	0.1030	24.9314	0.0228	25.0001	2.011e-05
	50	49.407	0.1976	50.2708	0.0903	49.9576	0.0141	50	1.0137e-12
	100	100.022	0.0072	99.763	0.0792	99.9722	0.0092	99.9999	2.6598e-05
	150	150.1628	0.0543	150.214	0.0713	149.9867	0.0044	149.9999	3.439e-05
	200	200	0.0001	199.807	0.0643	199.9823	0.0059	199.9999	1.8124e-05
	250	250.1813	0.0604	250.344	0.1146	249.9968	0.0010	250	5.2207e-06
	275	275.25	0.833	275.206	0.0686	275.023	0.0076	275	8.7713e-06
	295	294.994	0.0020	294.233	0.0344	295.0023	0.00076	295	5.5303e-06
AB	5	5.126	0.0419	4.819	0.0602	4.9302	0.0232	5.0002	5.7939e-05
	25	25.141	0.0470	25.0437	0.0146	24.9558	0.0147	25.0001	2.7364e-05
	50	50.122	0.0470	50.1416	0.0472	50.0224	0.0074	50	1.5608e-12
	100	100.032	0.0107	100.2485	0.0828	99.9618	0.0127	99.9999	3.2253e-05
	150	150.123	0.0410	149.9928	0.0024	149.9842	0.0052	149.9999	3.6227e-05
	200	199.992	0.0027	200.0953	0.0318	199.979	0.0070	199.9999	1.7065e-05
	250	250.201	0.0670	250.205	0.0683	250.0014	0.0004	250	4.8256e-06
	275	275.165	0.0550	276.182	0.3941	275.0126	0.0042	275	8.5677e-06
	295	294.996	0.0013	295.147	0.0489	295.0105	0.0035	295	6.045e-06

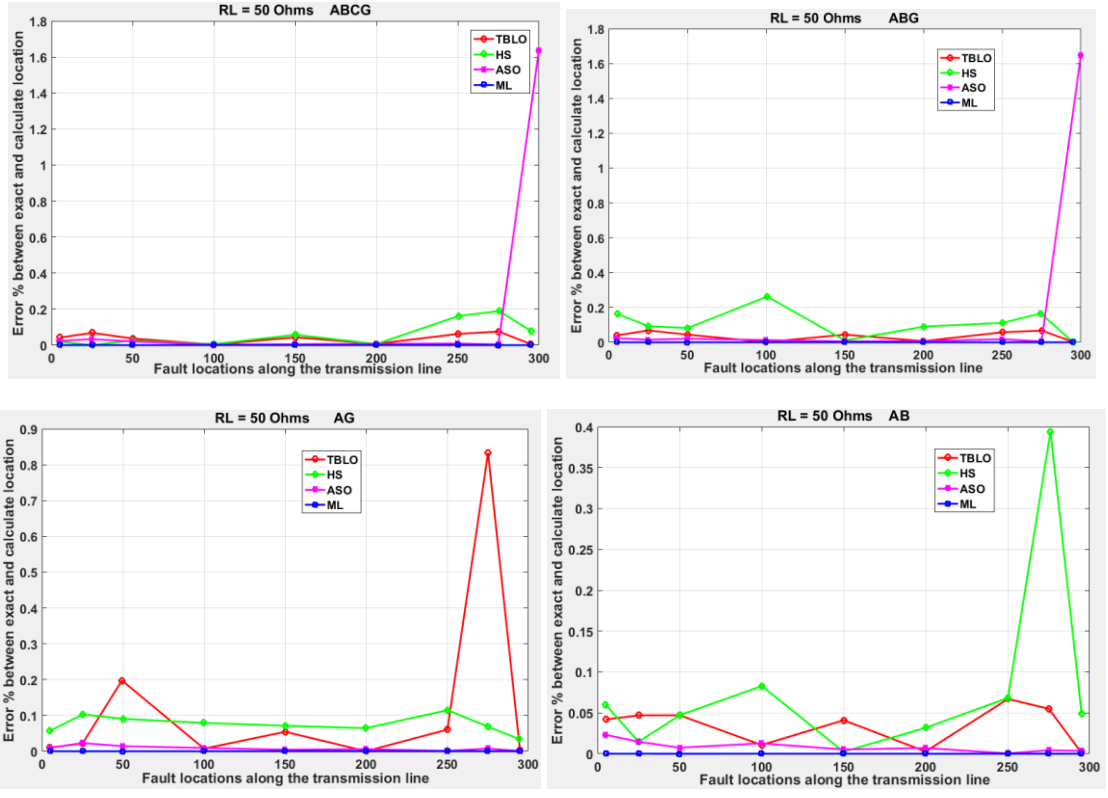

Fig. 7 – TBLO, HS, ASO, and ML fault location results along the transmission line with different fault locations and fault resistance R_L = 50 Ω.

It is observed that the ASO algorithm is completely independent of fault resistance, as the behavior is consistent with all fault resistance values and types, except for values (ABCG and ABG R_L = 50), which can be considered out of range. One of the most important points to mention here is that the ML algorithm is independent of fault resistance and fault type along the transmission line, and it does not affect its accuracy in fault location detection.

4.1. IMPACT OF FAULT RESISTANCE

Fault resistance significantly affects the accuracy of double-ended fault location methods. To assess the effectiveness of the proposed algorithms under varying fault resistances (RL), simulations were conducted with different fault resistance values of RL (1 Ω, 10 Ω, and 50 Ω). The parameters of the remote source impedance remained constant, and fault distances varied from 1 km to 300 km. The calculation error of fault location under different RL scenarios is summarized in Tables 2–4. The maximum error observed was 1.6469 % when RL was 50 Ω. Notably, the accuracy remained relatively consistent regardless of RL. The three scenarios' results affirm the proposed methods' acceptable accuracy.

4.2. OUTCOME FOR DIFFERENT FAULT TYPES

The effectiveness of the proposed methods extends beyond single-phase-to-ground faults, encompassing various fault types. This study evaluates the application of the methods under different fault scenarios, including single-phase, two-phase, two-phase-to-ground, and three-phase faults. For the simulations, the fault resistance (R_L) was configured at 1 Ω, 10 Ω, and 50 Ω, while the fault distance (y) ranged from 1 km to 300 km. The values of the remote system impedance and other parameters were kept constant. The accuracy of fault location remains consistent across these fault types, as demonstrated by the results in Tables 1,2 and 3.

4.3. DISCUSSION

Tables 1 through 3 present the outcomes of the proposed techniques (ML & ASO) and methods proposed in the existing literature (HS & TLBO). These results encompass fault types, distinct fault locations, and fault resistances. The data illustrates that ML exhibits a significantly high precision in identifying fault locations and boasts the advantage of not relying on specific initial conditions to initiate iterations. In contrast, a notable limitation of ASO, HS, and TLBO lies in their dependence on initial conditions, which can be a significant drawback.

The fault is situated at a distance of 250 km from the A terminal. In this scenario, ML demonstrated its precision by pinpointing the fault's location at 249.999 km from the A terminal, which is exceptionally close to the accurate location
with an error percentage of only $4.2674.10^{-5}$ %. This performance surpasses ASO, HS, and TLBO, which registered error percentages of 0.0087 %, 0.1038 %, and 0.1296 % respectively. Machine learning (ML) consistently exhibited highly accurate fault location results, irrespective of the fault type (A-B-C-G, A-B-G, A-B, and A-G), regardless of the fault resistance.

Table 4

Comparison of the four algorithms in terms of timing considerations with variation of fault resistance.

Method	R_L = 1 Ω	R_L = 10 Ω	R_L = 50 Ω
TLBO [1]	15s	/	7s
HS [1]	45s	/	/
ASO	90s	90s	90s
ML (spline)	2s	2s	2s

In the case of other methods, as the fault resistance rises, it gradually impacts the detection accuracy, leading to an increase in error from 0.02 % to 0.1 %. However, this increment in error remains quite insignificant. Table 4 compares the four algorithms above in terms of calculation time, confirming that the ML algorithm is the most efficient for estimating fault locations as it requires less time for calculation.

Table 5 illustrates the comparison among the four algorithms mentioned in terms of average percentage error, revealing that the accuracy and percentage error of the three methods are nearly equivalent. However, the ML method offers superior localization precision, resulting in an almost negligible error.

Table 5

Comparison of the four algorithms based on the average percentage error for different fault resistance values

Method	R_L = 1 Ω	R_L = 10 Ω	R_L = 50 Ω
TLBO [1]	0.024 %	0.024 %	0.0680 %
HS [1]	0.0177 %	0.0145 %	0.0680 %
ASO	0.0164 %	0.0216 %	0.7942 %
ML (spline)	2.7821e-05 %	1.9963e-05%	2.20e-05 %

5. **CONCLUSION**

The paper discusses how the ASO and ML techniques equip power systems with reliable tools for fault detection and location. The first algorithm (ASO) relies on post-fault data to formulate an optimization problem, subsequently optimized using specialized techniques. The second method employs machine learning, drawing from historical fault data. The ASO algorithm demonstrates high accuracy but requires approximately 90 s to determine fault locations, whereas the ML algorithm achieves the best accuracy in a significantly shorter timeframe, around 0.2 s. Consequently, both methods exhibit minimal error in fault location even when faced with fault type or resistance alterations. Given the critical importance of swift fault resolution, The ML algorithm highlights the improvement in fault detection accuracy and reduced computational time compared to traditional methods.

Recent applications of the ML algorithm across diverse electrical engineering domains highlight its success. The escalating adoption of both basic and modified versions of the ML algorithm attests to its potential and efficacy. It's noteworthy that building the necessary database for machine learning demands substantial time investment. Future efforts could explore using linear machine learning (LML) and the hybridization between ASO and machine learning metaheuristics.

Received on 17 October 2023

APPENDIX A

The line parameters used in this study are provided in Table A1.

Table A1

Transmission line characteristics

Parameters	Positive sequence	Zero sequence
Resistance	27.5 mΩ/km	27.5 mΩ/km
Inductance	1.00268 mH/km	3.26798 mH/km
Capacity	0.013 μF/km	0.0085 μF/km

REFERENCES

1. A.S. Ahmed, M.A. Attia, N.M. Hamed, A.Y. Abdelaziz, *Modern optimization algorithms for fault location estimation in power*

systems, Engineering Science and Technology, an International Journal, **20**, pp. 1475–1485 (2017).
2. J. Ezquerra, V. Valverde, A.J. Mazon, I. Zamora and J.J. Zamora, *Field programmable gate array implementation of a fault location system in transmission lines based on artificial neural networks*, IET Generation, Transmission & Distribution, **5**, *2*, pp. 191–198 (2011).
3. C.E.M. Pereira, L.C. Zanetta, *Fault location in transmission lines using one-terminal postfault voltage data*, IEEE Transactions Power Delivery, **19**, pp. 570–575 (2004).
4. L. Wei, W. Guo, F. Wen, G. Ledwich, Z. Liao, J. Xin, *Waveform Matching Approach for Fault Diagnosis of a High-Voltage Transmission Line Employing Harmony Search Algorithm*, IET Generation, Transmission & Distribution, **4**, pp. 801–809 (2010).
5. M. Kezunovic, S. Lou, Z. Galijasevic, D. Ristanovic, *Accurate fault location in transmission networks using modeling, simulation and limited field recorded data*, Power Systems Engineering Research Center, pp. 1–50 (2002).
6. R. Rohani, A. Koochaki, J. Siahbalaee, *Fault location in VSC-HVDC systems based on NSGA-II and discrete wavelet transform*, International Journal of Renewable Energy Research, **12**, *3*, pp. 1347–1361 (2022).
7. S. G. Di Santo, A.D.R. Albertini, R.R. Tiferes, *Optimization-Based Fault Location Algorithm for Series-Compensated Power Transmission Lines*, IEEE Access, **10**, pp. 46864–46877 (2022).
8. H. Gupta, P. Kumar, S. Saurabh, S.K. Mishra, B. Appasani, A. Pati, C. Ravariu, A. Srinivasulu, *Category boosting machine learning algorithm for breast cancer prediction*, Rev. Roum. Sci. Techn. – Électrotechn. et Énerg, **66**, *3*, pp. 201–206 (2021).
9. F. Rafique, L. Fu, M.H.U. Haq, R. Mai, *Automatic features extraction by transfer learning for transmission line protection*, Rev. Roum. Sci. Techn– Électrotechn. et Énerg. **68**, *3*, pp. 339–344 (2023).
10. B. Ponnuswamy, C. Columbus, S.R. Lakshmi, J. Chithambaram, *Wind turbine fault modeling and classification using cuckoo-optimized modular neural networks*, Rev. Roum. Sci. Techn.– Électrotechn. et Énerg, **68**, *4*, pp. 369–374, (2023).
11. B.R.C. Joseph, I.J. Jebadurai, G.J.L. Paulraj, J. Jebadurai, *Mulli mary varuveL deep vein net: deep vein thrombosis identification via sooty tern optimized deep learning network*, Rev. Roum. Sci. Techn.–Électrotechn. et Énerg., **69**, *1*, pp. 115–120, 2024.
12. N. Sabri, A. Tlemçani, A. Chouder, *Real-time diagnosis of battery cells for stand-alone photovoltaic system using machine learning techniques*, Rev. Roum. Sci. Techn.–Électrotechn. et Énerg., **66**, *2*, pp. 105–110, 2021.
13. J. Liang, Tao. Xiaojie, Fu. Yang, Fu. Yong, Mi. Yang, Li. Zhenkun, *A new single ended fault location method for transmission line based on positive sequence superimposed network during auto-reclosing*, IEEE Transactions on Power Delivery, **34**, *3*, pp. 1019–1029 (2019).
14. Z. Weigu, W. Liying, Z. Zhenxing, *Atom search optimization and its application to solve a hydrogeologic parameter estimation problem*, Knowledge-Based Systems, **163**, *1*, pp. 283–304 (2019).
15. L. Roach, G.M. Rignanese, A. Erriguible, C. Aymonier, *Applications of machine learning in supercritical fluids research*, The Journal of Supercritical Fluids, **202**, pp. 1–28 (2023).
16. M.G. Davoudi, J. Sadeh, E. Kamyab, *Time domain fault location on transmission lines using genetic algorithm*, 11th International Conference on Environment and Electrical Engineering IEEE, Venice, Italy, pp. 1–6, 18–25 May 2012.